Journal of Virology

Virology | Full-Length Text

DYRK1A is a multifunctional host factor that regulates coronavirus replication in a kinase-independent manner

Zhen Fu,[1,2] Yixin Xiang,[1,2] Yanan Fu,[1,2] Zhelin Su,[1,2] Yubei Tan,[1,2] Mengfang Yang,[1,2] Yuanyuan Yan,[1,2] Hakimeh Baghaei Daemi,[1,2] Yuejun Shi,[1,2] Shengsong Xie,[3] Limeng Sun,[1,2] Guiqing Peng[1,2,4,5]

AUTHOR AFFILIATIONS See affiliation list on p. 17.

ABSTRACT Coronaviruses (CoVs) pose a major threat to human and animal health worldwide, which complete viral replication by hijacking host factors. Identifying host factors essential for the viral life cycle can deepen our understanding of the mechanisms of virus–host interactions. Based on our previous genome-wide CRISPR screen of α-CoV transmissible gastroenteritis virus (TGEV), we identified the host factor dual-specificity tyrosine phosphorylation-regulated kinase 1A (DYRK1A), but not DYRK1B, as a critical factor in TGEV replication. Rescue assays and kinase inhibitor experiments revealed that the effect of DYRK1A on viral replication is independent of its kinase activity. Nuclear localization signal modification experiments showed that nuclear DYRK1A facilitated virus replication. Furthermore, DYRK1A knockout significantly downregulated the expression of the TGEV receptor aminopeptidase N (*ANPEP*) and inhibited viral entry. Notably, we also demonstrated that DYRK1A is essential for the early stage of TGEV replication. Transmission electron microscopy results indicated that DYRK1A contributes to the formation of double-membrane vesicles in a kinase-independent manner. Finally, we validated that DYRK1A is also a proviral factor for mouse hepatitis virus, porcine deltacoronavirus, and porcine sapelovirus. In conclusion, our work demonstrated that DYRK1A is an essential host factor for the replication of multiple viruses, providing new insights into the mechanism of virus–host interactions and facilitating the development of new broad-spectrum antiviral drugs.

IMPORTANCE Coronaviruses, like other positive-sense RNA viruses, can remodel the host membrane to form double-membrane vesicles (DMVs) as their replication organelles. Currently, host factors involved in DMV formation are not well defined. In this study, we used transmissible gastroenteritis virus (TGEV) as a virus model to investigate the regulatory mechanism of dual-specificity tyrosine phosphorylation-regulated kinase 1A (DYRK1A) on coronavirus. Results showed that DYRK1A significantly inhibited TGEV replication in a kinase-independent manner. DYRK1A knockout (KO) can regulate the expression of receptor aminopeptidase N (*ANPEP*) and endocytic-related genes to inhibit virus entry. More importantly, our results revealed that DYRK1A KO notably inhibited the formation of DMV to regulate the virus replication. Further data proved that DYRK1A is also essential in the replication of mouse hepatitis virus, porcine deltacoronavirus, and porcine sapelovirus. Taken together, our findings demonstrated that DYRK1A is a conserved factor for positive-sense RNA viruses and provided new insights into its transcriptional regulation activity, revealing its potential as a candidate target for therapeutic design.

KEYWORDS DYRK1A, coronavirus, virus entry, replication, double-membrane vesicle

Coronaviruses (CoVs) are a family of enveloped, positive, and single-stranded RNA viruses that can cause respiratory and intestinal diseases in both humans and a

Editor Tom Gallagher, Loyola University Chicago - Health Sciences Campus, Maywood, Illinois, USA

Address correspondence to Limeng Sun, Sunlimeng@webmail.hzau.edu.cn, or Guiqing Peng, penggq@mail.hzau.edu.cn.

The authors declare no conflict of interest.

See the funding table on p. 17.

Received 11 August 2023
Accepted 27 November 2023
Published 15 December 2023

variety of animals and can be divided into four genera: α, β, γ, and δ (1–3). Currently, seven coronaviruses that can infect humans have been identified (4). Severe acute respiratory coronavirus 2 (SARS-CoV-2), which belongs to the betacoronavirus genus, is currently receiving the most attention and poses a major threat to global public health (5, 6). In addition, porcine transmissible gastroenteritis virus (TGEV), which belongs to the alphacoronavirus genus, can cause highly contagious intestinal infections in pigs of different ages and breeds (7). TGEV is particularly harmful to newborn piglets within 2 weeks of birth, causing a mortality rate of up to 100% (8). The high mutability of RNA viruses and the wide range of coronavirus hosts complicate the prevention and control of coronaviruses.

Studies based on CRISPR screening have bridged the research gap in determining mechanisms of virus–host interactions and successfully identified host genes required for multiple viruses (9–14). For example, mucins are identified as a prominent viral restriction network that inhibits SARS-CoV-2 and diverse respiratory viruses (14). mLST8 is reported to regulate autophagy through the mTORC1 pathway and affect double-membrane vesicle (DMV) formation to regulate coronavirus replication (15). It has also been reported that host kinases play pivotal roles in viral replication. For instance, glycogen synthase kinase-3 is critical for CoV nucleocapsid (N) protein phosphorylation and function in the virus life cycle (16). Receptor for activated protein C kinase 1 is a host factor required for Zika virus (ZIKV) replication and is involved in the formation of viral replication factories (17). These findings suggest that the investigation of virus–host interaction mechanisms responsible for virus replication may contribute to the development of potential host-targeted antiviral therapeutics.

DYRK1A encodes dual-specificity tyrosine phosphorylation-regulated kinase 1A, a member of the CMGC kinase group (18), which possesses serine and threonine phosphorylation activity as well as autophosphorylation activity at tyrosine residues (19, 20). DYRK1A has been reported to contain a nuclear localization signal (NLS) sequence, a protein kinase domain, a highly conserved 13-consecutive-histidine repeat, and a repeat of serine/threonine residues (21, 22). Since its discovery, DYRK1A has been considered a molecule associated with the pathogenesis of Down syndrome (23). With further research into the function of DYRK1A, it has been found to play important roles in the cell cycle (24), cell differentiation (25), apoptosis (26, 27), splicing regulation (28), and tumorigenesis (29). Many recent studies have identified it as a potential target for the treatment of neurodegenerative diseases and cancer (30, 31).

In the present study, we used TGEV as a model virus and identified DYRK1A as a critical host factor for coronavirus replication. We found that knocking out DYRK1A significantly inhibited virus replication in a kinase-independent manner and that the nuclear distribution of DYRK1A was essential for this process. DYRK1A knockout (KO) significantly reduced the expression of aminopeptidase N (ANPEP), the known functional receptor of TGEV (32, 33), and inhibited virus entry. Further experiments showed that DYRK1A knockout also strongly affected the replication stage of the virus, and DMV formation in DYRK1A KO cells was significantly reduced, as determined by transmission electron microscopy (TEM) experiments. We further illustrated that DYRK1A KO also exhibits an inhibitory effect against mouse hepatitis virus (MHV), porcine deltacoronavirus (PDCoV), and porcine sapelovirus (PSV). In conclusion, our study suggests that DYRK1A represents a promising broad-spectrum target against positive-sense virus infection.

RESULTS

DYRK1A, but not DYRK1B, is a host factor required for TGEV replication

We identified DYRK1A as a critical host factor for TGEV based on a genome-wide CRISPR/Cas9 screen in porcine kidney-15 cells (PK-15 cells). To validate the potential effect of DYRK1A on TGEV replication, we generated a DYRK1A KO PK-15 cell line using the CRISPR/Cas9 gene editing system. Sanger sequencing (Fig. S1A) and western blotting (Fig. 1A) confirmed the successful construction of the DYRK1A KO cell line. In addition,

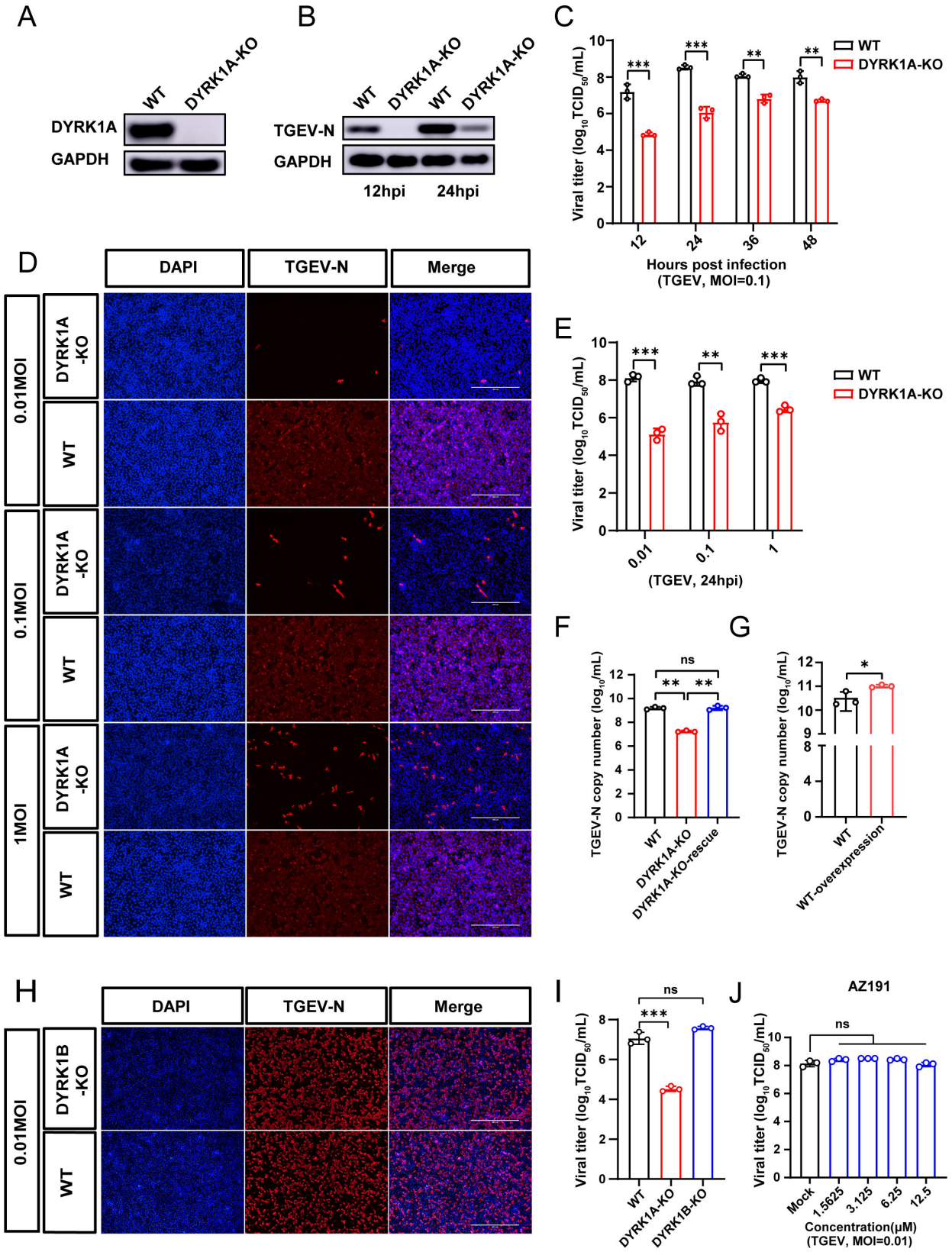

FIG 1 DYRK1A, but not DYRK1B, is a host factor essential for TGEV replication. (A) Western blot analysis validated the protein expression level of endogenous DYRK1A in DYRK1A KO cells and WT cells. GAPDH was used as an internal control gene. (B) Western blot assay to detect the TGEV N protein expressed in DYRK1A KO and WT cells following infection with TGEV [multiplicity of infection (MOI) = 0.1], at 12 and 24 hours post-infection (hpi). GAPDH was used as an internal

(Continued on next page)

FIG 1 (Continued)

control gene. (C) Multiple step viral growth assay. The viral titers in DYRK1A KO and WT cells infected with TGEV (MOI = 0.1) were monitored at different time points (12, 24, 36, and 48 h). (D and E) DYRK1A KO and WT cells were infected with TGEV at different MOIs (0.01, 0.1, and 1). Immunofluorescence assays (D) were used to detect the TGEV N protein expression following infection with TGEV at 24 hpi. Scale bar, 400 µm. TGEV titers (E) were tested at 24 hpi. (F) Rescue assays for WT, DYRK1A KO, and DYRK1A KO-rescue cells infected with TGEV (MOI = 0.1) at 24 hpi. The TGEV N copy number was assessed by quantitative real-time PCR. (G) Overexpression of DYRK1A in PK-15 control cells following infection with TGEV (MOI = 0.01) at 24 hpi. RT-qPCR assay for determination of the absolute mRNA level of the TGEV N gene. WT, transfection of the pcDNA3.1 empty vector in PK-15 cells; WT-overexpression, transfection of the pcDNA3.1-DYRK1A vector in PK-15 cells. (H and I) DYRK1B KO and WT cells were infected with TGEV (MOI = 0.01). Immunofluorescence assays (H) were used to detect TGEV N protein expression following infection with TGEV at 24 hpi. Scale bar, 400 µm. TGEV titers (I) were tested at 24 hpi. (J) PK-15 cells were incubated in advance with the DYRK1B inhibitor AZ191 at different concentrations (12.5, 6.25, 3.125, and 1.5625 µM) for 2 h, and the cells treated with the inhibitor were infected with TGEV (MOI = 0.01). The TGEV titers were tested at 24 hpi. The means and SDs of the results from three independent experiments are shown. ns, not significant; $^{*}P < 0.05$; $^{**}P < 0.01$; $^{***}P < 0.001$. *P*-values were determined by two-tailed unpaired Student's *t*-tests.

the proliferation of clonal DYRK1A KO cells and wild-type (WT) cells was measured, and no significant differences were detected by cell proliferation assays (MTS) (Fig. S1B).

We performed a western blot assay and found that the TGEV-encoded N protein was undetectable or weakly expressed in DYRK1A KO cells compared with WT cells at a MOI of 0.1 at 12 and 24 hpi (Fig. 1B). Further results showed that viral titers were reduced in the DYRK1A KO cells after TGEV infection, at 12, 24, 36, and 48 hpi, respectively (Fig. 1C). Meanwhile, immunofluorescence analysis (Fig. 1D) showed that DYRK1A KO cells possessed significantly diminished levels of TGEV N protein after infection with MOIs of 0.01, 0.1, and 1. Consistent with the immunofluorescence assay, the results of viral titer assays (Fig. 1E) at different MOIs showed significantly lower viral loads in DYRK1A KO cells than that in WT cells. These results revealed that the knockout of DYRK1A significantly inhibited TGEV replication. To further determine whether DYRK1A is required for TGEV infection, we constructed a CRISPR-resistant DYRK1A KO-rescue cell line, which stably expressed the DYRK1A gene on its KO cells, and its successful construction was verified by RT-qPCR (Fig. S1D) and western blot assay (Fig. S1F). As shown in Fig. 1F; Fig. S1C, the complementation of DYRK1A in DYRK1A KO cells fully restored TGEV replication. The overexpression of DYRK1A in WT cells also facilitated TGEV replication (Fig. 1G; Fig. S1E). Collectively, these results suggest that DYRK1A is a critical factor for TGEV infection.

Since DYRK1B is an important homologous protein of DYRK1A (34) and shares high similarity in structure as shown in Fig. S1H, we investigated whether DYRK1B plays a role in TGEV infection. A clonal DYRK1B KO cell line was generated through the CRISPR/Cas9 gene editing system, and Sanger sequencing (Fig. S1I) confirmed its successful construction. In contrast to DYRK1A KO cells, DYRK1B KO cells did not inhibit TGEV infection, as shown by immunofluorescence (Fig. 1H) and viral titer (Fig. 1I) assays. A highly selective inhibitor of DYRK1B, AZ191 (35), was used to further validate the effects of DYRK1B on TGEV. The results of the viral titer assay showed that it has no inhibitory effect on TGEV replication at tolerated concentrations (Fig. 1J; Fig. S1G). Therefore, our data indicate that DYRK1A, but not DYRK1B, is an essential factor for TGEV replication.

DYRK1A promotes TGEV replication in a kinase-independent manner

DYRK1A kinase has been reported to phosphorylate both nuclear and cytoplasmic proteins that are associated with multiple pathways (28, 36–40). To investigate whether DYRK1A kinase activity is related to the regulation of TGEV replication, we stably expressed full-length DYRK1A and the DYRK1A-K188R kinase-dead mutant (19) by lentiviral transduction in DYRK1A KO cells. Western blot results showed the successful complementation of DYRK1A and DYRK1A-K188R mutant in DYRK1A KO cells (Fig. 2A). Virus titer results revealed that the complementation of DYRK1A-K188R kinase-dead mutant restored viral infection to an extent similar to that with DYRK1A (Fig. 2B). To further validate whether the kinase activity of DYRK1A is essential to virus infection, Harmine (41) and INDY (42), two kinase inhibitors targeting DYRK1A, were applied at tolerated concentrations. Cell proliferation was not affected after treatment of certain concentrations of inhibitors as determined by the MTS assay (Fig. 2C and E). Consistent

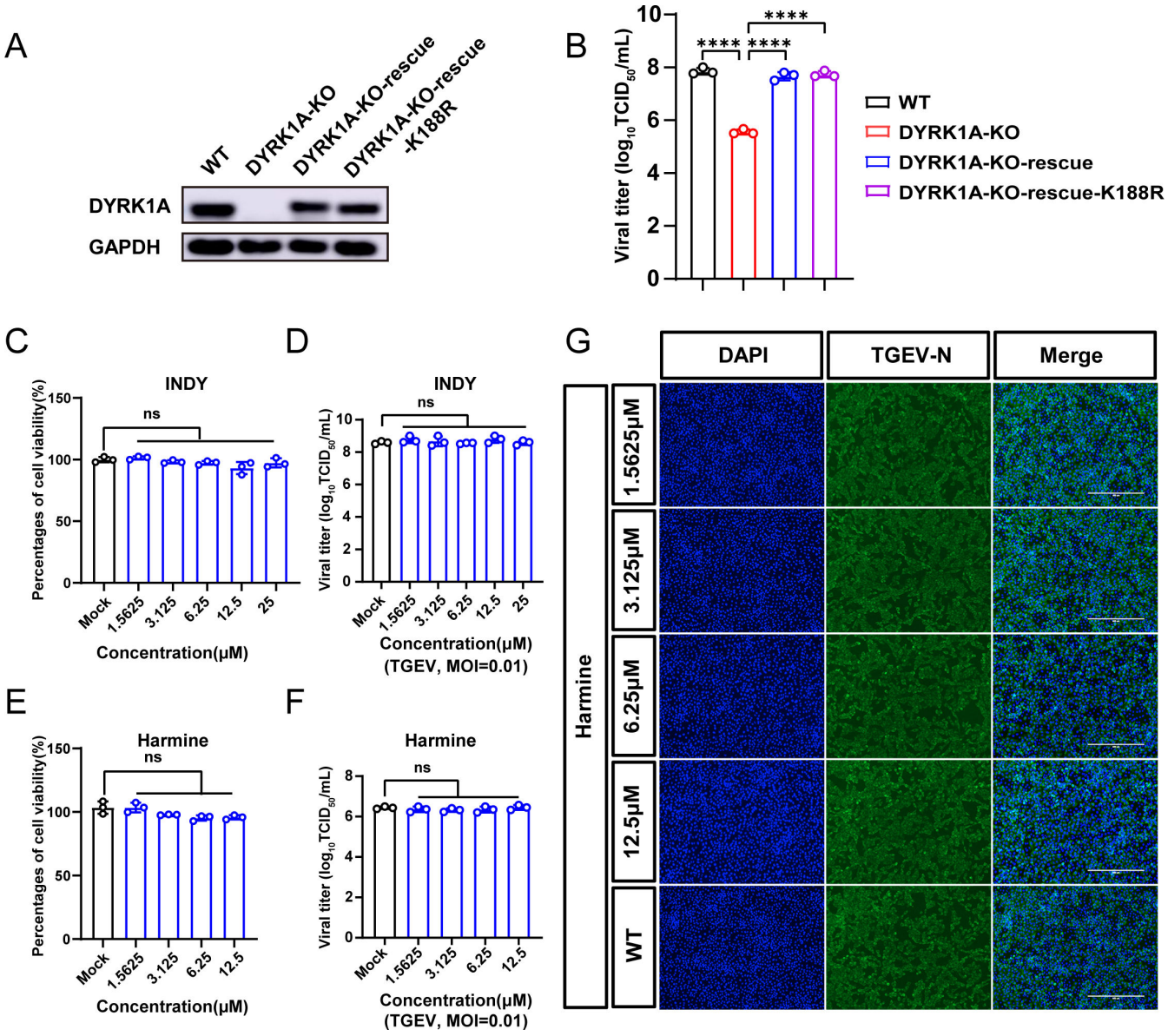

FIG 2 DYRK1A regulates TGEV replication independent of its kinase activity. (A) Western blot analysis validated the protein expression level of DYRK1A in WT, DYRK1A KO, DYRK1A KO-rescue, and DYRK1A KO-rescue-K188R cells. GAPDH was used as an internal control gene. (B) Rescue assays for WT, DYRK1A KO, DYRK1A KO-rescue, and DYRK1A KO-rescue-K188R cells infected with TGEV (MOI = 0.01). Viral titers were tested at 24 hpi. (C and E) PK-15 cells were treated with or without INDY (C) and Harmine (E) for 48 h, and cell viability was measured by the MTS assay. (D) PK-15 cells were incubated in advance with different concentrations (25, 12.5, 6.25, 3.125, and 1.5625 μM) of INDY for 2 h, and cells treated with the inhibitor were infected with TGEV (MOI = 0.01). The TGEV titers were tested at 24 hpi. (F and G) PK-15 cells were incubated in advance with different concentrations (12.5, 6.25, 3.125, and 1.5625 μM) of Harmine for 2 h, and cells treated with the inhibitor were infected with TGEV (MOI = 0.01). The TGEV titers (F) were tested at 24 hpi. The TGEV N protein was detected by the immunofluorescence assay (G). Scale bar, 400 μm. The means and SD of the results from three independent experiments are shown. $^{*}P < 0.05$; $^{**}P < 0.01$; $^{****}P < 0.0001$. *P*-values were determined by two-tailed unpaired Student's *t*-tests.

with the rescue assay, these kinase inhibitors exhibited no antiviral effect on TGEV as determined by virus titers (Fig. 2D and F) and immunofluorescence assays (Fig. 2G). Overall, these results highlight that DYRK1A regulates TGEV replication in a kinase-independent manner.

Nuclear DYRK1A facilitates TGEV replication

DYRK1A is predominantly nucleus-localized, but its cytoplasmic distribution has also been reported (43, 44). The wide distribution in the nucleoplasm may be related to the various physiological functions of DYRK1A. Our confocal microscopy results showed that DYRK1A in PK-15 cells is distributed in the nucleus, with a partial distribution in the cytoplasm (Fig. 3A). In the viral infection process, we found that DYRK1A is mostly concentrated in the nucleus after viral infection, with little cytoplasmic distribution (Fig. 3A). We then investigated whether the nucleoplasmic localization of DYRK1A is essential for virus replication. A nuclear localization mutant DYRK1A-ΔNLS was constructed as

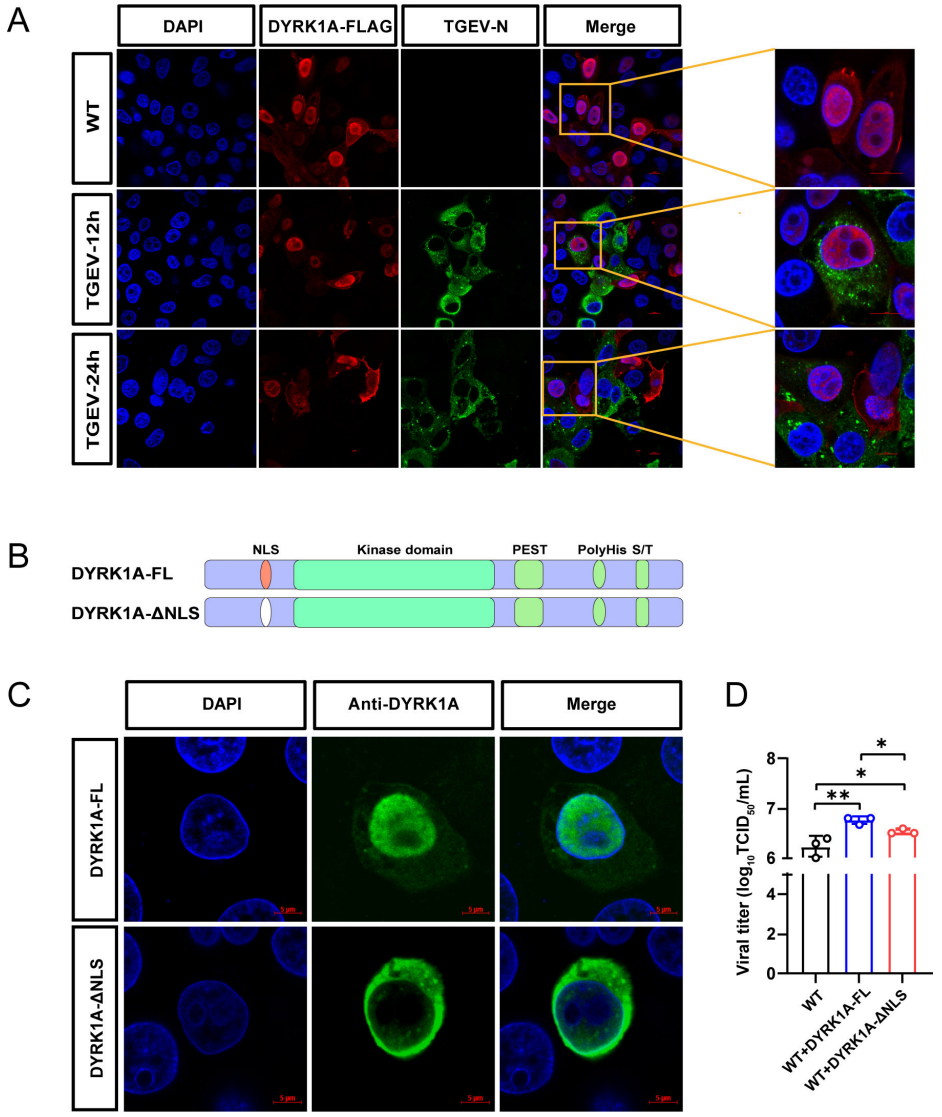

FIG 3 Nucleus-located DYRK1A facilitates TGEV replication. (A) Confocal fluorescence microscopy analysis of the subcellular localization of TGEV N (indicated in green) and ectopic expression of DYRK1A-FLAG (indicated in red) in WT cells mock-infected (above) or infected with TGEV (MOI = 1), at 12 hpi (middle) and 24 hpi (bottom). Scale bar, 10 µm. (B) Schematic representation of the construction of full-length DYRK1A (above) and DYRK1A-ΔNLS mutant (DYRK1A with deletion of the nuclear localization motif) (bottom). (C) Assessment of the subcellular location of ectopically expressed full-length DYRK1A (above) and DYRK1A-ΔNLS (bottom) (indicated in green) in WT cells via confocal fluorescence microscopy. Scale bar, 5 µm. (D) Overexpression of full-length DYRK1A and DYRK1A-ΔNLS in PK-15 control cells following infection with TGEV (MOI = 0.01). TGEV titers were tested at 24 hpi. The means and SD of the results from three independent experiments are shown. $^{*}P < 0.05$; $^{**}P < 0.01$. *P*-values were determined by two-tailed unpaired Student's *t*-tests.

indicated in Fig. 3B, and confocal experiments showed the distinct distribution of full-length DYRK1A and the DYRK1A-ΔNLS mutant (Fig. 3C). The viral titer assay showed that the overexpression of full-length DYRK1A promoted TGEV replication in WT cells (Fig. 3D). However, the ability to promote TGEV replication was reduced when DYRK1A-ΔNLS was overexpressed in WT cells compared with full-length DYRK1A. Taken together, these data indicate that nuclear DYRK1A can promote viral replication.

DYRK1A KO inhibits TGEV entry by downregulating the expression of ANPEP

Considering its strong effect on TGEV infection, we sought to explore which stage of the virus infection cycle is affected in DYRK1A KO cells. The attachment assay (Fig. 4A) and internalization assay (Fig. 4B) showed that DYRK1A KO suppressed virus entry. Membrane fusion assays (Fig. 4C) indicated that the ability of the TGEV spike protein to fuse to the TGEV receptor ANPEP was significantly reduced in DYRK1A KO cells compared to WT cells. Further RNA sequencing (RNA-Seq) analysis (Fig. 4D; Table S1) and RT-qPCR validation results (Fig. 4E) revealed a notable decline in the mRNA transcript level of *ANPEP* in the absence of DYRK1A, which may explain the viral entry impairment. The rescue assay showed that the *ANPEP* mRNA level was restored to the WT level upon reintroduction of DYRK1A and the DYRK1A-K188R mutant. Moreover, analysis of differentially expressed genes (DEGs) and RT-qPCR assays also revealed that loss of DYRK1A resulted in lower mRNA expression levels of endocytosis-related genes, such as *CPED1, DAB2, EGF, THRB, AMPH,* and *MAP2K6* (Fig. 4F).

To further verify whether the antiviral effect of DYRK1A KO is mediated exclusively by the downregulation of the receptor ANPEP, we constructed ANPEP-overexpressing DYRK1A KO cells. RT-qPCR results showed the successful overexpression of ANPEP on DYRK1A KO cells (Fig. 4G). Further validation determined by attachment and internalization experiments showed that the impaired virus entry was completely restored up to WT levels by the overexpression of ANPEP in DYRK1A KO cells (Fig. 4H and I). We then tested the TGEV replication, and the viral titer assay showed that the viral replication in ANPEP-overexpressing DYRK1A KO cells, though slightly higher than DYRK1A KO cells, was still impaired compared with WT cells (Fig. 4J). The above data suggest that DYRK1A KO inhibits TGEV entry by downregulating ANPEP expression, but the effect of DYRK1A on the virus is not restricted to the entry phase.

Overall, DYRK1A may intricately regulate transcription and gene expression to support viral entry independent of its kinase activity, and further research on the mechanism of how DYRK1A regulates gene expression may also be of appreciable importance.

DYRK1A KO inhibits the viral RNA synthesis in TGEV replication stage by suppressing DMV formation

A TEM experiment was performed to directly observe the assembly of virus particles and further investigate the mechanism by which DYRK1A knockout inhibits viral replication. Numerous vesicle-wrapped virus-like particles were detected in WT cells, whereas virions were rarely observed in DYRK1A KO cells after virus infection, suggesting that virion production was significantly impaired in the cells lacking DYRK1A (Fig. 5A). Subsequently, the release assay (Fig. 5B) showed that the extracellular and intracellular viral titers of DYRK1A KO cells were approximately equal, and both were lower than those of WT cells, indicating that DYRK1A KO does not affect TGEV release. We then wanted to investigate the effects of knocking out DYRK1A on viral genome replication. The confocal microscopy assay was performed to assess early replication, and the results showed that double-stranded RNA (dsRNA) replication intermediates were greatly decreased in abundance in DYRK1A KO cells compared to WT cells at 3 hpi (Fig. 5C). Moreover, strand-specific quantitative real-time PCR (RT-qPCR) was performed to detect the synthesis of positive-strand and negative-strand viral RNA (+vRNA and −vRNA, respectively) at different time points after viral infection. The level of positive-strand and negative-strand RNA synthesis was significantly lower in DYRK1A KO cells than that

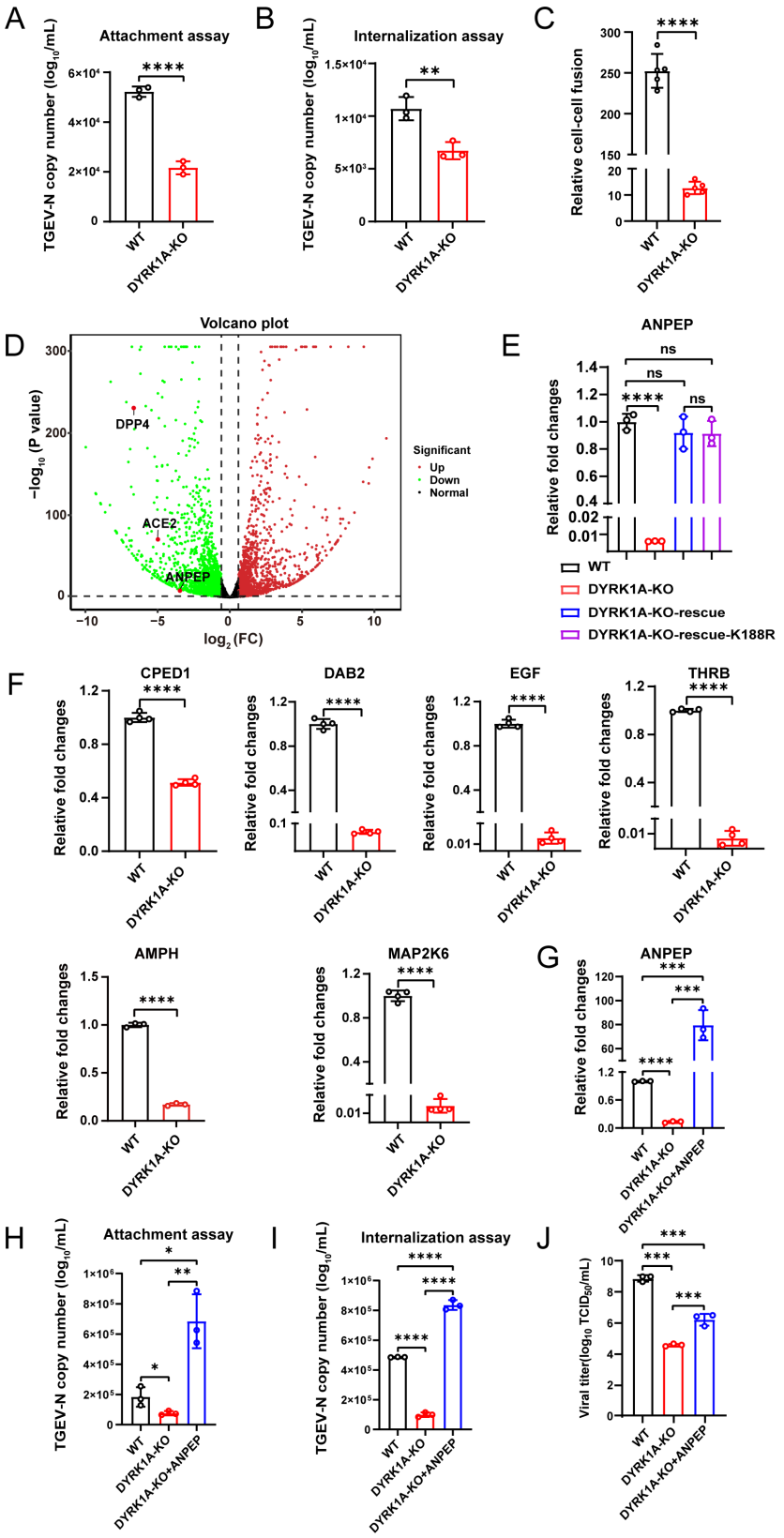

FIG 4 Knockout of DYRK1A inhibits TGEV entry by downregulating the expression of ANPEP. (A) DYRK1A KO and WT cells were infected with TGEV (MOI = 50) at 4°C for 1 h and assessed for TGEV adsorption. The cells were harvested, and viral RNA was extracted to determine virion attachment at the cell surface.

(Continued on next page)

FIG 4 (Continued)

(B) DYRK1A KO and WT cells were infected with TGEV (MOI = 50) at 4°C for 1 h, followed by incubation at 37°C for 30 min. The internalization of TGEV in DYRK1A KO and WT cells was evaluated by absolute quantitative real-time PCR. (C) Membrane fusion assay assessed the fusion ability of the TGEV spike protein in WT cells and DYRK1A KO cells. (D) Volcano plot of differentially expressed genes in WT and DYRK1A KO PK-15 cells. The expression of *ANPEP*, *ACE2*, and *DPP4* was strongly reduced in the absence of DYRK1A. (E) RT-qPCR assay for determination of relative mRNA levels of ANPEP in WT, DYRK1A KO, DYRK1A KO-rescue, and DYRK1A KO-rescue-K188R cells. (F) RT-qPCR validation of mRNA expression of endocytic pathway genes enriched according to RNA-seq. (G) RT-qPCR assay for determination of relative mRNA levels of ANPEP in WT, DYRK1A KO, and ANPEP-overexpressing DYRK1A KO cells. (H) WT, DYRK1A KO, and ANPEP-overexpressing DYRK1A KO cells were infected with TGEV (MOI = 50) at 4°C for 1 h and assessed for TGEV adsorption by RT-qPCR assay. (I) WT, DYRK1A KO, and ANPEP-overexpressing DYRK1A KO cells were infected with TGEV (MOI = 50) at 4°C for 1 h, followed by incubation at 37°C for 30 min. The internalization of TGEV was evaluated by absolute quantitative real-time PCR. (**J**) WT, DYRK1A KO, and ANPEP-overexpressing DYRK1A KO cells were infected with TGEV (MOI = 0.01). Viral titers were tested at 24 hpi. The means and SD of the results from three independent experiments are shown. $^{*}P < 0.05$; $^{**}P < 0.01$; $^{***}P < 0.001$; $^{****}P < 0.0001$. *P*-values were determined by two-tailed unpaired Student's *t*-tests.

in WT cells from 4 hpi onward (Fig. 5D). Furthermore, to bypass the viral entry stage, TGEV-bacterial artificial chromosome (BAC) was transfected into DYRK1A KO and WT cells to assess the difference in viral replication. RT-qPCR results showed that the RNA synthesis of TGEV was significantly lower in DYRK1A KO cells than that in WT cells, and this effect could be rescued to WT levels by the stable supplementation of DYRK1A and DYRK1A-K188R mutant in DYRK1A KO cells (Fig. 5E). These findings indicated that RNA synthesis was severely impaired in the absence of DYRK1A, confirming that DYRK1A is necessary for viral RNA replication.

Coronavirus can reshape host cell membranes to form its replication organelle DMV and provide a propitious environment for viral RNA synthesis (45, 46). TEM results showed that numerous typical DMVs (150–300 nm in diameter) were readily observed in infected WT cells (Fig. 5F), which were irregular in shape and often contained fibrous contents (47). In contrast with typical DMVs found in infected WT cells, the number of DMV was severely reduced in DYRK1A KO cells (Fig. 5F and G). Instead, a large number of monolayered vesicles of varying morphology and size were observed in DYRK1A KO cells after virus infection. TEM experiments also showed that even in ANPEP-overexpressing DYRK1A KO cells, DMV formation was impaired, and the number of DMV was still reduced compared to WT cells. Remarkably, DMV formation was readily observed in DYRK1A KO cells complemented with both DYRK1A and the DYRK1A-K188R kinase-dead mutant (Fig. 5F and G), suggesting that DYRK1A plays a crucial role in DMV formation in a kinase-independent manner. Taken together, these results indicate that DYRK1A KO can inhibit the early replication of TGEV by suppressing DMV formation and viral RNA synthesis.

DYRK1A is a host factor for the replication of multiple viruses

Given that DYRK1A is highly conserved in eukaryotic cells and has important physiological functions (48), we speculated that DYRK1A may be a broad-spectrum host factor during infection for multiple viruses. DYRK1A KO clones in murine fibroblast cell line (L929) were generated to test whether DYRK1A can regulate betacoronavirus mouse hepatitis virus A-59 infection. Sanger sequencing confirmed the successful knockout of DYRK1A in L929 cells (Fig. S2A). The loss of DYRK1A did not affect cell viability in L929 cells as measured by the MTS assay (Fig. S2B). Further RT-qPCR assay (Fig. S2C) and western blotting assay (Fig. S2D) revealed that the expression of the functional receptor of MHV, carcinoembryonic antigen-related cellular adhesion molecule 1 (CEACAM1) (49, 50), was notably reduced in DYRK1A KO L929 cells compared with WT cells. Compared with that in WT L929 cells, the viral titer was significantly decreased in DYRK1A KO cells (Fig. 6A). We further examined the necessity of DYRK1A for PDCoV and found that the virus titer in DYRK1A KO cell cultures was significantly reduced compared with that in

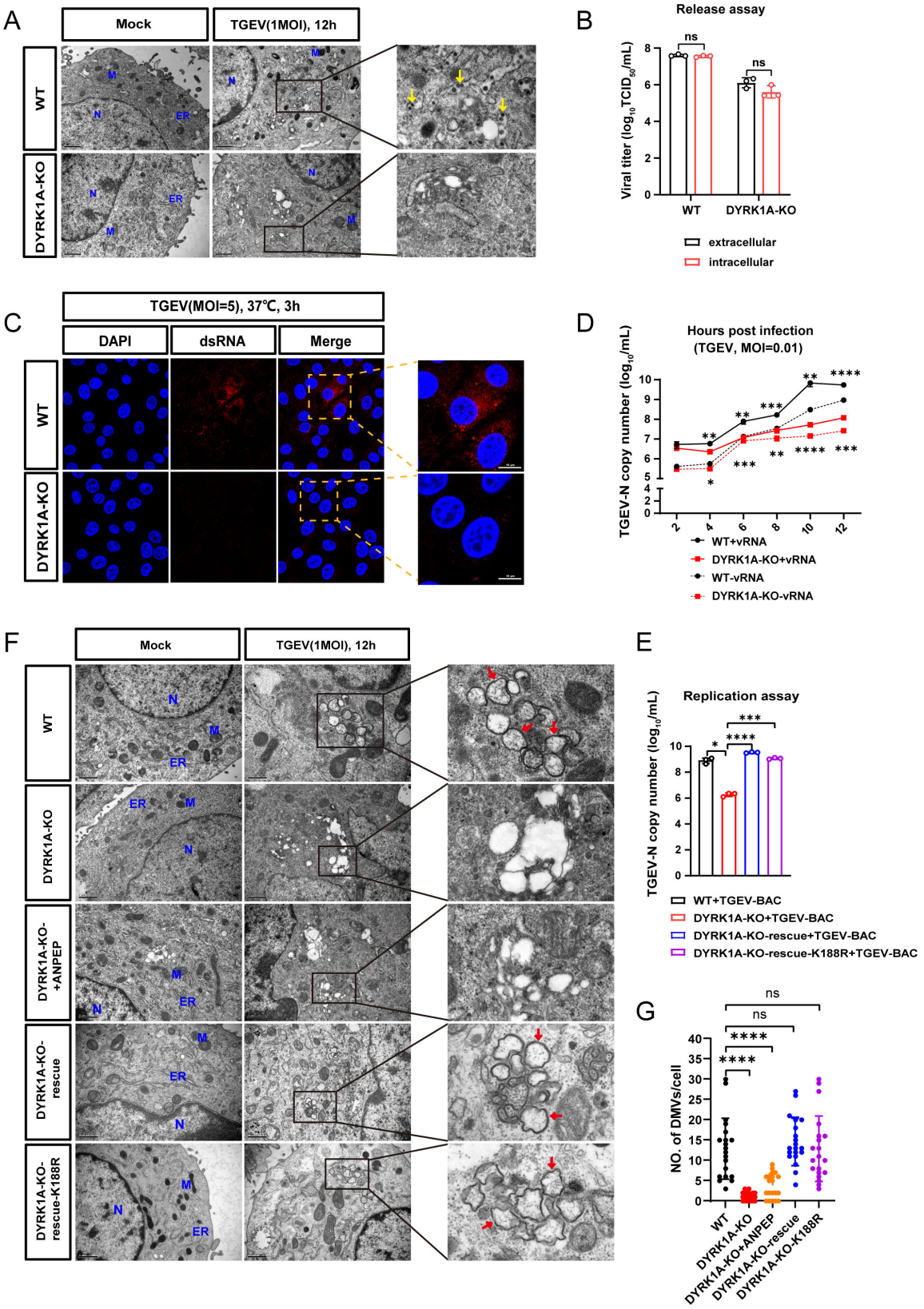

FIG 5 DYRK1A KO inhibits viral RNA synthesis of TGEV by suppressing DMV formation. (A) Evaluation of the effects of DYRK1A KO on virus particle assembly by TEM experiment. Compared with numerous virions (yellow arrows) found in WT cells, few virus-like particles wrapped in vesicles of varying sizes were found in DYRK1A KO cells. Scale bars, 1 µm or 500 nm. Mock, uninfected cells; M, mitochondria; ER, endoplasmic reticulum; N, nucleus. (B) Assessment of the TGEV

(Continued on next page)

FIG 5 (Continued)

release stage in DYRK1A KO and WT cells infected with TGEV (MOI = 0.1). Intracellular and extracellular viral titers were evaluated by virus median tissue culture infectious dose ($TCID_{50}$) assays at 24 hpi. (C) Confocal microscopy to evaluate early-stage TGEV replication by detecting dsRNA formation in WT and DYRK1A KO cells infected with TGEV (MOI = 5) at 3 hpi. Scale bars, 10 µm. (D) DYRK1A KO and WT cells were infected with TGEV at an MOI of 0.01. Positive (+vRNA) or negative (−vRNA) viral RNA was quantified by RT-qPCR. (E) Infectious TGEV-BAC plasmids were transfected into WT, DYRK1A KO, DYRK1A KO-rescue, and DYRK1A KO-rescue-K188R cells. After 8 h, they were incubated with an anti-TGEV S protein antibody, and after 48 h, the cells were collected and subjected to RT-qPCR. (F) Evaluation of DMV formation in WT, DYRK1A KO, ANPEP-overexpressing DYRK1A KO, DYRK1A KO-rescue, and DYRK1A KO-rescue-K188R cells by transmission electron microscopy. Numerous typical DMVs (diameter 150–300 nm) were observed in TGEV-infected PK-15 cells, DYRK1A KO-rescue cells, and DYRK1A KO-rescue-K188R cells (MOI = 1, 12 hpi) (red arrows). TGEV-infected DYRK1A KO and ANPEP-overexpressing DYRK1A KO cells contained several monolayer vesicles. Scale bar, 1 µm or 500 nm as indicated. (G) Quantification of DMV numbers per cell is shown as the mean ± SD (n = 20). The means and SD of the results from three independent experiments are shown. $^{*}P < 0.05$; $^{**}P < 0.01$; $^{***}P < 0.001$; $^{****}P < 0.0001$. P-values were determined by two-tailed unpaired Student's t-tests.

WT cell cultures (Fig. 6B). In addition, we validated that DYRK1A KO significantly reduced the replication ability of PSV, another positive-sense RNA virus, as measured by the virus titer assay (Fig. 6C). Moreover, we also tested whether DYRK1A affects the replication of vesicular stomatitis virus (VSV), which is a negative-sense RNA virus, and found that the virus titers in the supernatant of DYRK1A KO cells showed no difference from those in WT cells (Fig. 6D). Furthermore, the results of the virus titer assay revealed that DYRK1A KO had no resistant effect on pseudorabies virus (PRV) (Fig. 6E), a member of DNA virus. These results suggested that DYRK1A may be a host factor broadly required for the replication of positive-sense RNA viruses. In summary, during replication, viruses may utilize DYRK1A to regulate the expression of virus entry-related genes to facilitate virus entry through its transcriptional regulatory activity. DYRK1A also plays an important role in DMV formation and thus affects viral RNA synthesis. Overall, as shown in diagram Fig. 6F, we indicated that DYRK1A KO inhibits the entry and replication stage of the coronavirus life cycle.

DISCUSSION

Coronaviruses pose a severe threat to human and animal health worldwide. Relevant studies to elucidate CoV–host interactions and develop new drug targets against emerging infectious diseases are urgently needed. Our CRISPR screen modeled on TGEV identified DYRK1A as a top-ranked host factor (51). In the present study, we validated that DYRK1A participates in the replication of α-, β-, and δ-group CoVs. Several independent CRISPR screens have also revealed that DYRK1A is a host factor required for human CoVs, such as SARS-CoV-2 (12–14), MERS-CoV (13), HCoV-229E, and HCoV-NL63 (10), suggesting that DYRK1A plays an important conserved role in the infection of viruses throughout the coronavirus family and is valuable for mechanistic studies.

Our experimental results demonstrated that DYRK1A, but not DYRK1B, is required for TGEV infection. DYRK1A and DYRK1B belong to the class I DYRK1 family, with 85% homology in the kinase active region, while there are major differences outside the catalytic domain (21), which may explain their different effects on viral replication. For instance, DYRK1A has a unique polyhistidine repeat sequence at its C-terminus, which is absent in DYRK1B. The histidine repeats of DYRK1A were reported to act as a speckle-targeting signal, and DYRK1A overexpression can induce speckle disassembly to further regulate transcription (44, 52, 53). DYRK1A has been reported to regulate transcription activity that is not entirely dependent on its kinase activity. Specifically, protein interactions and promoter regulation are also important in the transcriptional regulation by DYRK1A, particularly under conditions where kinase activity is not essential (54, 55). Our rescue experiments and inhibitor treatment assays showed that viral replication is not dependent on the kinase activity of DYRK1A, which is consistent with a previous report (56). Nuclear cytoplasmic trafficking has been reported to be an important mechanism to modulate transcription factor function (57). Our nucleocytoplasmic migration and localization experiments demonstrated the importance and necessity of DYRK1A nuclear localization for viral replication. Therefore, it is reasonable to

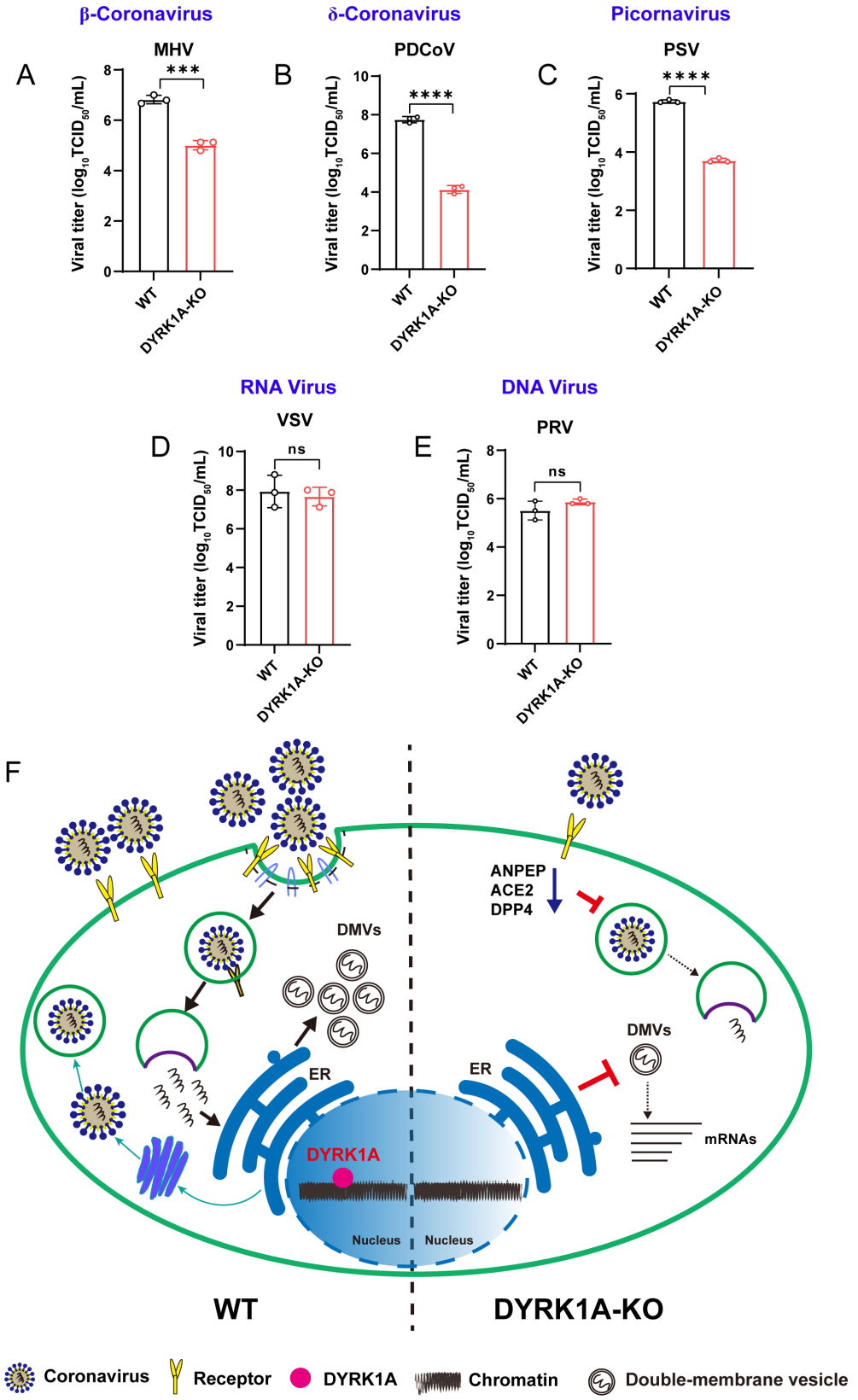

FIG 6 DYRK1A is a host factor for multiple viruses. (A) WT and DYRK1A KO L929 cells were infected with MHV (MOI = 0.01), and the MHV titers were tested at 18 hpi. (B and C) WT and DYRK1A KO PK-15 cells were infected with (B) PDCoV (MOI = 0.1, 24 hpi) and (C) PSV (MOI = 0.1, 24 hpi). Viral titers were measured by $TCID_{50}$ assays. (D and E) WT and DYRK1A KO PK-15 cells

(Continued on next page)

FIG 6 (Continued)

were infected with (D) VSV (MOI = 0.01, 24 hpi) and (E) PRV (MOI = 0.01, 36 hpi). Viral titers were measured by $TCID_{50}$ assays. (F) A model illustrating the roles of DYRK1A in the CoV replication cycle. In WT cells, CoV binds to its receptor and enters the cell through clathrin- and caveolin-mediated endocytosis and then releases its genome into the cytoplasm after membrane fusion in the early/late endosome. In DYRK1A KO cells, the expression of receptor and endocytic-related genes was reduced, resulting in impaired viral entry. Moreover, DMV formation in DYRK1A KO cells was suppressed, leading to the inhibition of virus replication. Data are representative of at least three independent experiments. $^{***}P < 0.001$; $^{****}P < 0.0001$. *P*-values were determined by two-tailed unpaired Student's *t*-tests.

hypothesize that DYRK1A's transcriptional regulation, independent of its kinase activity, is responsible for the effects on viral replication. However, the exact mechanisms still need further exploration.

A previous study indicated that DYRK1A can regulate *ACE2* and *DPP4* transcription in primate cells by altering chromatin accessibility in a kinase-independent manner (56). In the present study, we revealed that DYRK1A can positively regulate the expression of *ANPEP* to affect TGEV entry in PK-15 cells independent of kinase activity. Notably, we also observed a significant reduction in the expression of coronavirus entry-related receptor genes such as *ACE2* and *DPP4* in PK-15 cells lacking DYRK1A, supporting a conserved transcriptional regulation role for DYRK1A. ANPEP has been identified as a co-receptor facilitating PDCoV infection (58–61), suggesting a possible mechanism by which DYRK1A could influence PDCoV entry. The expression of CEACAM1, a functional receptor for MHV, was found notably reduced in DYRK1A KO L929 cells, indicating a role of DYRK1A for MHV entry regulation. As for porcine sapelovirus, it is known to recognize α2, 3-linked sialic acid on GD1a ganglioside as its receptor (62). However, whether DYRK1A regulates this interaction remains unclear. We hypothesize that DYRK1A could regulate the expression of CoV receptors to influence virus entry.

Coronaviruses are positive single-strand RNA viruses that replicate in the cytoplasm by reshaping host cell membranes to induce DMVs as replication organelles (45, 63). Our study revealed that DYRK1A KO can inhibit viral RNA synthesis by suppressing DMV formation independent of its catalytic activity, which has not yet been reported. DYRK1A primarily localizes in the nucleus, yet it acts as a potent host factor with wide-ranging transcriptional regulatory effects, capable of modulating proteins in both the nucleus and cytoplasm (54–56, 64–67). Our RNA sequencing also demonstrated that DYRK1A influences a diverse array of host factors that are involved in multiple pathways (Table S1). We hypothesize that DYRK1A may indirectly regulate DMV biogenesis through the transcriptional regulation of host factors required for DMV formation and, therefore, influence virus replication. Considering that positive-strand RNA viruses require the hijacking of host membranes to form DMVs as their replication organelles (45, 68, 69), we propose that DYRK1A may act as a conserved host factor in the replication of these viruses (Fig. 6A through C). The exact regulation by which this occurs is not particularly clear, and further study is required to elucidate the specific mechanisms.

In summary, we have proposed a hypothetical model to illustrate the role of DYRK1A in the virus life cycle. As shown in Fig. 6F, DYRK1A KO downregulated the expression of viral entry-related genes, resulting in impaired virus entry. In addition, the formation of DMV was also severely impaired, and viral RNA synthesis was markedly reduced in the absence of DYRK1A. Taken together, our findings suggest that DYRK1A exhibits a broad spectrum of antiviral effects against positive-strand RNA viruses and provide new insights into its transcriptional regulatory activity, revealing its potential as a candidate therapeutic strategy against various emerging and re-emerging viruses.

MATERIALS AND METHODS

Plasmid construction

To construct the lentivirus sgRNA expression vector, the lenti-sgRNA-EGFP vector was digested by the *Bbs*I restriction enzyme (NEB), and the lentiCRISPR-v2 vector was digested by the *BsmB*I restriction enzyme (NEB). Individual sgRNAs were cloned into the lenti-sgRNA-EGFP vector and lentiCRISPR-v2 vector for validation in PK-15 cells and L929 cells, respectively. For rescue and overexpression experiments, to exclude the role of sgRNA and Cas9 in DYRK1A KO cells, DYRK1A was mutated at a specific base in the protospacer adjacent motif sequence, which did not alter the encoded amino acid. A point mutation was induced in the sequence of DYRK1A, and the mutant sequence was cloned into the pLVX-T2A-mCherry-Puro vector (Clontech), which was digested with *Xho*I and *BamH*I. The sequences of amino acid site (K188R) mutated in DYRK1A were cloned into a pLVX-T2A-mCherry-Puro vector to construct DYRK1A kinase-dead mutant for restoration experiments. Sanger sequencing (Tsingke) was performed to confirm all plasmids. All primer sequences are listed in Table S2.

Cell culture and viruses

The PK-15 and HEK293T cell lines were purchased from the Cell Bank of the Chinese Academy of Sciences (Shanghai, China). The L929 (CCL-1) line was purchased from ATCC (USA). All cell lines were then subjected to mycoplasma detection. For cell culture experiments in the present study, all cells were cultured in Dulbecco's modified Eagle's medium (DMEM) supplemented with 10% fetal bovine serum (FBS), 100 U/mL penicillin, and 100 µg/mL streptomycin and maintained at 37°C with 5% CO_2. The following viruses were used: TGEV WH-1 strain (GenBank accession no. HQ462571.1), PDCoV strain CHN-HN-2014 (GenBank accession no. KT336560), and MHV A59 strain (GenBank accession no. MF618253.1). VSV and PRV were provided by Prof. Gang Cao at Huazhong Agricultural University. TGEV, PDCoV, PSV, VSV, and PRV were propagated in PK-15 cells. MHV was propagated in L929 cells.

Viral titers

Candidate gene KO cells and WT cells were inoculated with virus in 24-well plates in triplicate. Cells were harvested at the indicated time points, and viral titers were determined on the basis of $TCID_{50}$ using corresponding sensitive cells.

Transfection and infection

All cell transfections were performed with the jetPRIME (Polyplus) reagent according to the manufacturer's instructions. For viral infections, WT and gene KO PK-15 cells were grown to approximately 80% confluency in a 12-well plate and incubated with TGEV at 37°C for 1 h. After adsorption, the cells were washed with phosphate-buffered saline (PBS), which was replaced with fresh medium supplemented with 2% FBS, followed by incubation at 37°C in 5% CO_2 for the indicated times. Infection was subsequently monitored by immunofluorescence assays and RT-qPCR assays.

Construction of candidate gene KO and stable gene rescue cell lines

The sgRNA lentivirus corresponding to each candidate gene was transduced into PK-15-Cas9 cells. After 72 h of transfection, cells with green fluorescent protein expression were enriched by fluorescence-activated cell sorting. To generate rescue cell lines, DYRK1A KO cells were transfected with lentivirus containing full-length DYRK1A with site-specific mutations. After 72 h of transfection, cells with mCherry expression were identified by fluorescence-activated cell sorting. The expression of the add-back DYRK1A gene was confirmed by western blot.

Western blotting and antibodies

Cells were lysed in cell lysis buffer containing 1× protease inhibitor (Beyotime) for 30 minutes at 4°C, and cellular debris was removed via centrifugation (12,000 × *g* for 15 minutes at 4°C). The lysed cells were denatured with SDS by heating at 95°C for 10 minutes, followed by incubation on ice for 5 minutes. Proteins were separated by SDS-PAGE and transferred onto a polyvinylidene fluoride membrane. Membranes were blocked with 5% milk in TBST for at least 3 h and incubated with primary antibody at 4°C overnight in 5% milk TBST. Membranes were washed 3× with TBST and incubated with secondary antibodies for 1 h at room temperature. Primary antibodies used for western blot include DYRK1A (Santa Cruz Biotechnology, sc-100376, 1:1,000) and GAPDH (Beyotime, no. AF5009, 1:5,000). Secondary antibodies include anti-mouse (Abbkine, no. A21010) and anti-rabbit (Abbkine, no. A21020) and were applied at 1:5,000 and 1:10,000 dilutions, respectively, in TBST for 1 h at room temperature. Proteins were detected with ECL Prime western blot detection reagents (GE Healthcare, United Kingdom).

RT-qPCR

Total RNA was extracted from cells with the TRIzol reagent (Invitrogen). Complementary DNAs (cDNAs) were synthesized using the PrimeScript RT Reagent Kit with gDNA Eraser (TaKaRa) in a total volume of 10 µL. Each RT-qPCR reaction was carried out with 100 ng of cDNA and 5 nM primer pairs by using SYBR Green Mix (Bio-Rad, USA). The results were monitored using a CFX96 Real-Time PCR Detection System (Bio-Rad, USA) programmed for one cycle of 15 minutes at 95°C, followed by 39 cycles of 10 seconds at 95°C and 30 seconds at 60°C. The relative expression levels were calculated using the $2^{-\Delta\Delta Ct}$ method. The Bbeta-actin gene was used as a normalization control. For absolute RT-qPCR, approximately 1 µL of viral RNAs was used as the template to synthesize cDNAs. Absolute RT-qPCR assays were performed using SYBR Green Mix and primers specific for the N gene of TGEV in a final reaction volume of 10 µL. The TGEV N protein-coding cDNA sequence from GenBank (accession number: ADY39745.1) was cloned into the pcDNA3.1 vector and used as an internal reference for the quantification of TGEV copy numbers. All primers used in quantitative PCR are listed in Table S2.

Immunofluorescence assay

The protein expression levels of TGEV N protein in candidate gene KO cells and control cells were determined via the immunofluorescence assay. Cells were infected with TGEV at different MOI values. Then, the cells were washed with PBS at 24 hpi. Subsequently, the cells were fixed with 4% paraformaldehyde for 30 minutes at room temperature, permeabilized with 0.3% Triton X-100 in PBS for 10 minutes, and then washed three times with 1× PBS. The permeabilized cells were blocked for 30 minutes with PBS containing 5% bovine serum albumin. Cells were incubated with TGEV N antibody (the rabbit anti-TGEV N protein polyclonal antibody was prepared in our laboratory) or anti-dsRNA antibody (SCICONS, no. 10010200, 1:1,000) at 37°C for 2 h. Before incubation with the secondary antibody, the cells were washed three times with PBS for 10 minutes each. The secondary antibodies were Alexa Fluor 594 goat anti-mouse IgG (H + L) (Invitrogen, no. A-11005, 1:1,000) and Alexa Fluor 594 anti-rabbit IgG (H + L) (Invitrogen, no. A-11012, 1:1,000), and the cells were incubated at 37°C for 1 h. Finally, the samples were washed three times with PBS, and the cell nuclei were counterstained with 4′,6-diamidino-2-phenylindole (DAPI) (Sigma, no. D9542) at room temperature for 2 minutes. The incubation with secondary antibodies and DAPI was carried out in the dark. Cell samples were observed and imaged with a fluorescence microscope (Thermo Fisher Scientific EVOS FL Auto).

MTS assay

To assess cell viability and cell proliferation, MTS proliferation assays were performed. The MTS assay was performed using the MTS assay kit (Abcam, no. ab197010). Cells were

seeded into 96-well plates and incubated for 12 h. The culture medium was replaced with the fresh medium that contained the compounds at different concentrations and incubated continuously for 48 h. Afterward, 10 µL of the MTS reagent was directly added to each well and incubated for 2 h in standard culture conditions. The absorbance values of the cells at 490 nm were measured to determine cell viability.

TEM assay

Cells were infected with TGEV at an MOI of 1 for 12 h. The cells were washed three times with precooled PBS and fixed by adding 3 mL of 2.5% glutaraldehyde (Servicebio) at room temperature for 2 h. After fixation, cells were transferred to a 2 mL centrifuge tube. TEM samples were performed by Servicebio Company, and images were taken using an HZAU TEM platform (HITACHI, no. H-7650).

RNA sequencing and transcriptome analysis

For high-throughput RNA-seq, RNA libraries were created from each group, such as DYRK1A KO cells (i.e., DYRK1A_KO_MOCK and DYRK1A_KO_TGEV) and WT cells (i.e., WT_MOCK and WT_TGEV). Three replicates were conducted for each sample. Poly(A) + RNA isolation, library construction, and sequencing were performed using BMKCloud (www.biocloud.net). Illumina NovaSeq 6000 was used to sequence the constructed library. Raw data (raw reads) of FASTQ format were processed through in-house perl scripts. All the downstream analyses were based on clean data with high quality. These clean reads were then mapped to the reference genome sequence. Hisat2 tools soft were used to map with the reference genome. DEGs were obtained by DESeq2 (v1.30.1) with a *P*-value cutoff ≤0.05 and an absolute fold change of ≥1.5.

Drug treatment assay

Harmine (cat. no. HY-N0737A), INDY (cat. no. HY-108476), and AZ191 (cat. no. HY-12277) were purchased from MedChemExpress and dissolved in dimethyl sulfoxide at a stock concentration of 10 mM and then frozen in aliquots at −80°C. Cells were incubated with the specified concentration of inhibitor for 2 h and then infected with TGEV at an MOI of 0.01. Then, the cells were prepared for immunofluorescence assays at 24 hpi, and the supernatants were collected for viral titer assays.

Virion attachment and internalization assay

WT and DYRK1A KO cells were infected with TGEV (MOI = 50) and incubated at 4°C for 1 h. For the virus attachment assay, cells were washed three times with cold PBS (at 4°C) to remove unbound viral particles and harvested to extract viral RNA. The amount of viral RNA was determined by RT-qPCR. For the internalization assay, the infected cells described above were further cultured with prewarmed DMEM at 37°C for another 1 h. Subsequently, the cells were treated with acidic PBS-HCl (pH 3.0) to remove the attached but uninternalized viral particles. After washing three times, the cells were lysed with the TRIzol reagent to extract total RNA, and the viral RNA was quantified by RT-qPCR.

Membrane fusion assay

A luciferase-based quantitative assay was used to measure the efficiency of cell–cell fusion mediated by TGEV S protein on WT and DYRK1A KO cells as previously described (70). The effector cells, 293T cells, were co-transfected with the plasmids expressing TGEV S proteins and the plasmids encoding the fusion protein with the GAL4 DNA binding domain and the NF-κB transcription activation domain. The target cells, WT and DYRK1A KO cells, were transfected with the plasmids encoding a luciferase reporter gene under the control of a synthetic promoter with five tandem repeats of the yeast GAL4 binding sites. At 24 h post-transfection, effector and target cells were cocultured at a 1:1 ratio for 24 h. The cell–cell fusion activity was expressed as the relative activity of firefly luciferase.

Confocal microscopy

To observe the endocytosis of the TGEV in host cells, the same amount of DYRK1A KO cells and control cells were cultured in 35 mm Petri dishes overnight. An equivalent dose of TGEV (MOI = 5) was added to each well and incubated at 4°C for 60 minutes for complete adsorption and then transferred to 37°C and incubated for 30 minutes for endocytosis. Immunofluorescence assays were performed as described above, while the images were acquired using a laser scanning confocal microscope (Nikon). The subcellular localization of DYRK1A in DYRK1A KO cells and control cells transfected with DYRK1A-FLAG-pcDNA3.1 plasmid was observed after 24 h. Afterward, TGEV (MOI = 1) was added into these cells, incubated for 24 h, immunolabeled with a FLAG-tag antibody (Proteintech, no. 20543-1-AP; MBL, no. PM020) and dsRNA antibody (SCICONS, no. 10010200, 1:1,000), and imaged to identify double-fluorescent positive cells.

Statistical analysis

Statistical significance values were assessed using GraphPad Prism 8.0. Two-tailed unpaired *t*-tests were used for data analysis. Unless otherwise stated, the data represent the mean ± standard deviation of experiments performed, at least, in triplicate.

ACKNOWLEDGMENTS

We thank Jianbo Cao and Limin He (Huazhong Agricultural University) for TEM support. We also thank Yan Wang and Yuan Sun (Institute of Hydrobiology, Chinese Academy of Sciences) for flow cytometry technical support.

The study was supported by the National Science Fund for Distinguished Young Scholars (Grant No. 32125037) and the National Natural Science Foundation of China (Grant No. 32202784).

AUTHOR AFFILIATIONS

[1]State Key Laboratory of Agricultural Microbiology, College of Veterinary Medicine, Huazhong Agricultural University, Wuhan, China
[2]Key Laboratory of Preventive Veterinary Medicine in Hubei Province, The Cooperative Innovation Center for Sustainable Pig Production, Wuhan, China
[3]Key Laboratory of Agricultural Animal Genetics, Breeding and Reproduction of Ministry of Education & Key Lab of Swine Genetics and Breeding of Ministry of Agriculture and Rural Affairs, Huazhong Agricultural University, Wuhan, China
[4]Key Laboratory of Prevention & Control for African Swine Fever and Other Major Pig Diseases, Ministry of Agriculture and Rural Affairs, Wuhan, China
[5]Hubei Hongshan Laboratory, Frontiers Science Center for Animal Breeding and Sustainable Production, Wuhan, China

AUTHOR ORCIDs

Zhen Fu http://orcid.org/0009-0000-5442-9812
Limeng Sun http://orcid.org/0000-0003-3884-3428
Guiqing Peng http://orcid.org/0000-0001-8813-6663

FUNDING

Funder	Grant(s)	Author(s)
MOST | National Natural Science Foundation of China (NSFC)	32202784	Limeng Sun
MOST | NSFC | National Science Fund for Distinguished Young Scholars (National Science Foundation for Distinguished Young Scholars)	32125037	Guiqing Peng

AUTHOR CONTRIBUTIONS

Zhen Fu, Conceptualization, Data curation, Investigation, Methodology, Software, Validation, Visualization, Writing – original draft, Writing – review and editing | Yixin Xiang, Data curation, Methodology, Validation, Writing – review and editing | Yanan Fu, Data curation, Methodology, Validation, Writing – review and editing | Zhelin Su, Formal analysis, Validation, Writing – review and editing | Yubei Tan, Methodology, Validation, Writing – review and editing | Mengfang Yang, Methodology, Software, Validation | Yuanyuan Yan, Methodology, Software, Validation | Hakimeh Baghaei Daemi, Methodology, Software, Writing – review and editing | Yuejun Shi, Methodology, Validation | Shengsong Xie, Methodology, Validation | Limeng Sun, Conceptualization, Methodology, Software, Validation, Writing – review and editing | Guiqing Peng, Conceptualization, Formal analysis, Funding acquisition, Project administration, Supervision

DATA AVAILABILITY

The data that support the findings of this study are openly available in this article and are available from the corresponding author upon request.

ADDITIONAL FILES

The following material is available online.

Supplemental Material

Supplemental figures (JVI01239-23-s0001.docx). Fig. S1 and S2.
Table S1 (JVI01239-23-s0002.xlsx). RNA-Seq analysis results.
Table S2 (JVI01239-23-s0003.xlsx). Primer list.

REFERENCES

1. González JM, Gomez-Puertas P, Cavanagh D, Gorbalenya AE, Enjuanes L. 2003. A comparative sequence analysis to revise the current taxonomy of the family coronaviridae. Arch Virol 148:2207–2235. https://doi.org/10.1007/s00705-003-0162-1
2. Masters PS. 2006. The molecular biology of coronaviruses. Adv Virus Res 66:193–292. https://doi.org/10.1016/S0065-3527(06)66005-3
3. Wong ACP, Li X, Lau SKP, Woo PCY. 2019. Global epidemiology of bat coronaviruses. Viruses 11:174. https://doi.org/10.3390/v11020174
4. Woo PCY, Lau SKP, Lam CSF, Lau CCY, Tsang AKL, Lau JHN, Bai R, Teng JLL, Tsang CCC, Wang M, Zheng B-J, Chan K-H, Yuen K-Y. 2012. Discovery of seven novel mammalian and avian coronaviruses in the genus deltacoronavirus supports bat coronaviruses as the gene source of alphacoronavirus and betacoronavirus and avian coronaviruses as the gene source of gammacoronavirus and deltacoronavirus. J Virol 86:3995–4008. https://doi.org/10.1128/JVI.06540-11
5. Deng S-Q, Peng H-J. 2020. Characteristics of and public health responses to the coronavirus disease 2019 outbreak in China. J Clin Med 9:575. https://doi.org/10.3390/jcm9020575
6. Zhou P, Yang XL, Wang XG, Hu B, Zhang L, Zhang W, Si HR, Zhu Y, Li B, Huang CL, et al. 2020. A pneumonia outbreak associated with a new coronavirus of probable bat origin. Nature 588:270–273. https://doi.org/10.1038/s41586-020-2951-z
7. Laude H, Rasschaert D, Delmas B, Godet M, Gelfi J, Charley B. 1990. Molecular biology of transmissible gastroenteritis virus. Vet Microbiol 23:147–154. https://doi.org/10.1016/0378-1135(90)90144-k
8. Moon HW, Norman JO, Lambert G. 1973. Age dependent resistance to transmissible gastroenteritis of swine (TGE). I. Clinical signs and some mucosal dimensions in small intestine. Can J Comp Med 37:157–166.
9. Schneider WM, Luna JM, Hoffmann HH, Sánchez-Rivera FJ, Leal AA, Ashbrook AW, Le Pen J, Ricardo-Lax I, Michailidis E, Peace A, Stenzel AF, Lowe SW, MacDonald MR, Rice CM, Poirier JT. 2021. Genome-scale identification of SARS-CoV-2 and pan-coronavirus host factor networks. Cell 184:120–132. https://doi.org/10.1016/j.cell.2020.12.006
10. Wang R, Simoneau CR, Kulsuptrakul J, Bouhaddou M, Travisano KA, Hayashi JM, Carlson-Stevermer J, Zengel JR, Richards CM, Fozouni P, Oki J, Rodriguez L, Joehnk B, Walcott K, Holden K, Sil A, Carette JE, Krogan NJ, Ott M, Puschnik AS. 2021. Genetic screens identify host factors for SARS-CoV-2 and common cold coronaviruses. Cell 184:106–119. https://doi.org/10.1016/j.cell.2020.12.004
11. Daniloski Z, Jordan TX, Wessels H-H, Hoagland DA, Kasela S, Legut M, Maniatis S, Mimitou EP, Lu L, Geller E, Danziger O, Rosenberg BR, Phatnani H, Smibert P, Lappalainen T, tenOever BR, Sanjana NE. 2021. Identification of required host factors for SARS-CoV-2 infection in human cells. Cell 184:92–105. https://doi.org/10.1016/j.cell.2020.10.030
12. Rebendenne A, Roy P, Bonaventure B, Chaves Valadão AL, Desmarets L, Arnaud-Arnould M, Rouillé Y, Tauziet M, Giovannini D, Touhami J, Lee Y, DeWeirdt P, Hegde M, Urbach S, Koulali KE, de Gracia FG, McKellar J, Dubuisson J, Wencker M, Belouzard S, Moncorgé O, Doench JG, Goujon C. 2022. Bidirectional genome-wide CRISPR screens reveal host factors regulating SARS-CoV-2, MERS-CoV and seasonal HCoVs. Nat Genet 54:1090–1102. https://doi.org/10.1038/s41588-022-01110-2
13. Wei J, Alfajaro MM, DeWeirdt PC, Hanna RE, Lu-Culligan WJ, Cai WL, Strine MS, Zhang S-M, Graziano VR, Schmitz CO, et al. 2021. Genome-wide CRISPR screens reveal host factors critical for SARS-CoV-2 infection. Cell 184:76–91. https://doi.org/10.1016/j.cell.2020.10.028
14. Biering SB, Sarnik SA, Wang E, Zengel JR, Leist SR, Schäfer A, Sathyan V, Hawkins P, Okuda K, Tau C, et al. 2022. Genome-wide bidirectional CRISPR screens identify mucins as host factors modulating SARS-CoV-2 infection. Nat Genet 54:1078–1089. https://doi.org/10.1038/s41588-022-01131-x
15. Fu Y, Fu Z, Su Z, Li L, Yang Y, Tan Y, Xiang Y, Shi Y, Xie S, Sun L, Peng G. 2023. Mlst8 is essential for coronavirus replication and regulates its replication through the mTORC1 pathway. mBio 14:e0089923. https://doi.org/10.1128/mbio.00899-23
16. Wu C-H, Yeh S-H, Tsay Y-G, Shieh Y-H, Kao C-L, Chen Y-S, Wang S-H, Kuo T-J, Chen D-S, Chen P-J. 2009. Glycogen synthase kinase-3 regulates the phosphorylation of severe acute respiratory syndrome coronavirus

nucleocapsid protein and viral replication. J Biol Chem 284:5229–5239. https://doi.org/10.1074/jbc.M805747200
17. Shue B, Chiramel AI, Cerikan B, To T-H, Frölich S, Pederson SM, Kirby EN, Eyre NS, Bartenschlager RFW, Best SM, Beard MR. 2021. Genome-wide CRISPR screen identifies RACK1 as a critical host factor for flavivirus replication. J Virol 95:e0059621. https://doi.org/10.1128/JVI.00596-21
18. Aranda S, Laguna A, de la Luna S. 2011. DYRK family of protein kinases: evolutionary relationships, biochemical properties, and functional roles. FASEB J 25:449–462. https://doi.org/10.1096/fj.10-165837
19. Himpel S, Panzer P, Eirmbter K, Czajkowska H, Sayed M, Packman LC, Blundell T, Kentrup H, Grötzinger J, Joost HG, Becker W. 2001. Identification of the autophosphorylation sites and characterization of their effects in the protein kinase DYRK1A. Biochem J 359:497–505. https://doi.org/10.1042/0264-6021:3590497
20. Walte A, Rüben K, Birner-Gruenberger R, Preisinger C, Bamberg-Lemper S, Hilz N, Bracher F, Becker W. 2013. Mechanism of dual specificity kinase activity of DYRK1A. FEBS J 280:4495–4511. https://doi.org/10.1111/febs.12411
21. Kentrup H, Becker W, Heukelbach J, Wilmes A, Schürmann A, Huppertz C, Kainulainen H, Joost H-G. 1996. DYRK, a dual specificity protein kinase with unique structural features whose activity is dependent on tyrosine residues between subdomains VII and VIII (*). J Biol Chem 271:3488–3495. https://doi.org/10.1074/jbc.271.7.3488
22. Song WJ, Sternberg LR, Kasten-Sportès C, Keuren ML, Chung SH, Slack AC, Miller DE, Glover TW, Chiang PW, Lou L, Kurnit DM. 1996. Isolation of human and murine homologues of the drosophila minibrain gene: human homologue maps to 21q22.2 in the down syndrome "critical region" Genomics 38:331–339. https://doi.org/10.1006/geno.1996.0636
23. Park J, Song WJ, Chung KC. 2009. Function and regulation of Dyrk1A: Towards understanding down syndrome. Cell Mol Life Sci 66:3235–3240. https://doi.org/10.1007/s00018-009-0123-2
24. Hille S, Dierck F, Kühl C, Sosna J, Adam-Klages S, Adam D, Lüllmann-Rauch R, Frey N, Kuhn C. 2016. DYRK1A regulates the cardiomyocyte cell cycle via D-cyclin-dependent Rb/E2f-signalling. Cardiovasc Res 110:381–394. https://doi.org/10.1093/cvr/cvw074
25. Soppa U, Schumacher J, Florencio Ortiz V, Pasqualon T, Tejedor FJ, Becker W. 2014. The down syndrome-related protein kinase DYRK1A phosphorylates p27(Kip1) and Cyclin D1 and induces cell cycle exit and neuronal differentiation. Cell Cycle 13:2084–2100. https://doi.org/10.4161/cc.29104
26. Seifert A, Allan LA, Clarke PR. 2008. DYRK1A Phosphorylates caspase 9 at an inhibitory site and is potently inhibited in human cells by Harmine. FEBS J 275:6268–6280. https://doi.org/10.1111/j.1742-4658.2008.06751.x
27. Laguna A, Aranda S, Barallobre MJ, Barhoum R, Fernández E, Fotaki V, Delabar JM, de la Luna S, de la Villa P, Arbonés ML. 2008. The protein kinase DYRK1A regulates caspase-9-mediated apoptosis during retina development. Dev Cell 15:841–853. https://doi.org/10.1016/j.devcel.2008.10.014
28. de Graaf K, Hekerman P, Spelten O, Herrmann A, Packman LC, Büssow K, Müller-Newen G, Becker W. 2004. Characterization of Cyclin L2, a novel Cyclin with an arginine/Serine-rich domain: Phosphorylation by Dyrk1A and Colocalization with splicing factors. J Biol Chem 279:4612–4624. https://doi.org/10.1074/jbc.M310794200
29. Fernández-Martínez P, Zahonero C, Sánchez-Gómez P. 2015. DYRK1A: the double-edged kinase as a protagonist in cell growth and tumorigenesis. Mol Cell Oncol 2:e970048. https://doi.org/10.4161/23723548.2014.970048
30. Abbassi R, Johns TG, Kassiou M, Munoz L. 2015. DYRK1A in neurodegeneration and cancer: molecular basis and clinical implications. Pharmacol Ther 151:87–98. https://doi.org/10.1016/j.pharmthera.2015.03.004
31. Ionescu A, Dufrasne F, Gelbcke M, Jabin I, Kiss R, Lamoral-Theys D. 2012. DYRK1A kinase inhibitors with emphasis on cancer. Mini Rev Med Chem 12:1315–1329. https://doi.org/10.2174/13895575112091315
32. Delmas B, Gelfi J, L'Haridon R, Vogel LK, Sjöström H, Norén O, Laude H. 1992. Aminopeptidase N is a major receptor for the entero-pathogenic coronavirus TGEV. Nature 357:417–420. https://doi.org/10.1038/357417a0
33. Luo L, Wang S, Zhu L, Fan B, Liu T, Wang L, Zhao P, Dang Y, Sun P, Chen J, Zhang Y, Chang X, Yu Z, Wang H, Guo R, Li B, Zhang K. 2019. Aminopeptidase N-null neonatal piglets are protected from transmissible gastroenteritis virus but not porcine epidemic diarrhea virus. Sci Rep 9:13186. https://doi.org/10.1038/s41598-019-49838-y
34. Papenfuss M, Lützow S, Wilms G, Babendreyer A, Flaßhoff M, Kunick C, Becker W. 2022. Differential maturation and chaperone dependence of the paralogous protein kinases DYRK1A and DYRK1B. Sci Rep 12:2393. https://doi.org/10.1038/s41598-022-06423-0
35. Ashford AL, Oxley D, Kettle J, Hudson K, Guichard S, Cook SJ, Lochhead PA. 2014. A novel DYRK1B inhibitor AZ191 demonstrates that DYRK1B acts independently of GSK3β to phosphorylate cyclin D1 at Thr(286), not Thr(288). Biochem J 457:43–56. https://doi.org/10.1042/BJ20130461
36. Woods YL, Rena G, Morrice N, Barthel A, Becker W, Guo S, Unterman TG, Cohen P. 2001. The kinase DYRK1A phosphorylates the transcription factor FKHR at Ser329 *in vitro*, a novel *in vivo* phosphorylation site. Biochem J 355:597–607. https://doi.org/10.1042/bj3550597
37. Mao J, Maye P, Kogerman P, Tejedor FJ, Toftgard R, Xie W, Wu G, Wu D. 2002. Regulation of gli1 transcriptional activity in the nucleus by DYRK1. J Biol Chem 277:35156–35161. https://doi.org/10.1074/jbc.M206743200
38. Chen-Hwang MC, Chen HR, Elzinga M, Hwang YW. 2002. Dynamin is a minibrain kinase/dual specificity Yak1-related kinase 1A substrate. J Biol Chem 277:17597–17604. https://doi.org/10.1074/jbc.M111101200
39. Matsuo R, Ochiai W, Nakashima K, Taga T. 2001. A new expression cloning strategy for isolation of substrate-specific kinases by using phosphorylation site-specific antibody. J Immunol Methods 247:141–151. https://doi.org/10.1016/s0022-1759(00)00313-6
40. Woods YL, Cohen P, Becker W, Jakes R, Goedert M, Wang X, Proud CG. 2001. The kinase DYRK Phosphorylates protein-synthesis initiation factor eIF2Bε at Ser539 and the microtubule-associated protein tau at Thr212: potential role for DYRK as a glycogen synthase kinase 3-priming kinase. Biochem J 355:609–615. https://doi.org/10.1042/bj3550609
41. Adayev T, Wegiel J, Hwang YW. 2011. Harmine is an ATP-competitive inhibitor for dual-specificity tyrosine phosphorylation-regulated kinase 1A (DYRK1A). Arch Biochem Biophys 507:212–218. https://doi.org/10.1016/j.abb.2010.12.024
42. Ogawa Y, Nonaka Y, Goto T, Ohnishi E, Hiramatsu T, Kii I, Yoshida M, Ikura T, Onogi H, Shibuya H, Hosoya T, Ito N, Hagiwara M. 2010. Development of a novel selective inhibitor of the down syndrome-related kinase DYRK1A. Nat Commun 1:86. https://doi.org/10.1038/ncomms1090
43. Becker W, Weber Y, Wetzel K, Eirmbter K, Tejedor FJ, Joost H-G. 1998. Sequence characteristics, subcellular localization, and substrate specificity of DYRK-related kinases, a novel family of dual specificity protein kinases. J Biol Chem 273:25893–25902. https://doi.org/10.1074/jbc.273.40.25893
44. Alvarez M, Estivill X, de la Luna S. 2003. DYRK1A accumulates in splicing speckles through a novel targeting signal and induces speckle disassembly. J Cell Sci 116:3099–3107. https://doi.org/10.1242/jcs.00618
45. Roingeard P, Eymieux S, Burlaud-Gaillard J, Hourioux C, Patient R, Blanchard E. 2022. The double-membrane vesicle (DMV): a virus-induced organelle dedicated to the replication of SARS-CoV-2 and other positive-sense single-stranded RNA viruses. Cell Mol Life Sci 79:425. https://doi.org/10.1007/s00018-022-04469-x
46. Knoops K, Kikkert M, Worm S van den, Zevenhoven-Dobbe JC, van der Meer Y, Koster AJ, Mommaas AM, Snijder EJ. 2008. SARS-coronavirus replication is supported by a reticulovesicular network of modified endoplasmic reticulum. PLoS Biol 6:e226. https://doi.org/10.1371/journal.pbio.0060226
47. Snijder EJ, van der Meer Y, Zevenhoven-Dobbe J, Onderwater JJM, van der Meulen J, Koerten HK, Mommaas AM. 2006. Ultrastructure and origin of membrane vesicles associated with the severe acute respiratory syndrome coronavirus replication complex. J Virol 80:5927–5940. https://doi.org/10.1128/JVI.02501-05
48. Deboever E, Fistrovich A, Hulme C, Dunckley T. 2022. The omnipresence of DYRK1A in human diseases. Int J Mol Sci 23:9355. https://doi.org/10.3390/ijms23169355
49. Hemmila E, Turbide C, Olson M, Jothy S, Holmes KV, Beauchemin N. 2004. Ceacam1a-/- mice are completely resistant to infection by murine coronavirus mouse hepatitis virus A59. J Virol 78:10156–10165. https://doi.org/10.1128/JVI.78.18.10156-10165.2004
50. Williams RK, Jiang GS, Holmes KV. 1991. Receptor for mouse hepatitis virus is a member of the carcinoembryonic antigen family of glycoproteins. Proc Natl Acad Sci U S A 88:5533–5536. https://doi.org/10.1073/pnas.88.13.5533

51. Sun L, Zhao C, Fu Z, Fu Y, Su Z, Li Y, Zhou Y, Tan Y, Li J, Xiang Y, Nie X, Zhang J, Liu F, Zhao S, Xie S, Peng G, Klein SL. 2021. Genome-scale CRISPR screen identifies TMEM41B as a multi-function host factor required for coronavirus replication. PLoS Pathog 17:e1010113. https://doi.org/10.1371/journal.ppat.1010113
52. Lamond AI, Spector DL. 2003. Nuclear speckles: a model for nuclear organelles. Nat Rev Mol Cell Biol 4:605–612. https://doi.org/10.1038/nrm1172
53. Salichs E, Ledda A, Mularoni L, Albà MM, de la Luna S. 2009. Genome-wide analysis of histidine repeats reveals their role in the localization of human proteins to the nuclear speckles compartment. PLoS Genet 5:e1000397. https://doi.org/10.1371/journal.pgen.1000397
54. Lepagnol-Bestel A-M, Zvara A, Maussion G, Quignon F, Ngimbous B, Ramoz N, Imbeaud S, Loe-Mie Y, Benihoud K, Agier N, Salin PA, Cardona A, Khung-Savatovsky S, Kallunki P, Delabar J-M, Puskas LG, Delacroix H, Aggerbeck L, Delezoide A-L, Delattre O, Gorwood P, Moalic J-M, Simonneau M. 2009. DYRK1A interacts with the REST/NRSF-SWI/SNF chromatin remodelling complex to deregulate gene clusters involved in the neuronal phenotypic traits of down syndrome. Hum Mol Genet 18:1405–1414. https://doi.org/10.1093/hmg/ddp047
55. von Groote-Bidlingmaier F, Schmoll D, Orth H-M, Joost H-G, Becker W, Barthel A. 2003. DYRK1 is a co-activator of FKHR (FOXO1a)-dependent glucose-6-phosphatase gene expression. Biochem Biophys Res Commun 300:764–769. https://doi.org/10.1016/s0006-291x(02)02914-5
56. Strine MS, Cai WL, Wei J, Alfajaro MM, Filler RB, Biering SB, Sarnik S, Chow RD, Patil A, Cervantes KS, Collings CK, DeWeirdt PC, Hanna RE, Schofield K, Hulme C, Konermann S, Doench JG, Hsu PD, Kadoch C, Yan Q, Wilen CB. 2023. DYRK1A promotes viral entry of highly pathogenic human coronaviruses in a kinase-independent manner. PLoS Biol 21:e3002097. https://doi.org/10.1371/journal.pbio.3002097
57. Hood JK, Silver PA. 1999. In or out? Regulating nuclear transport. Curr Opin Cell Biol 11:241–247. https://doi.org/10.1016/s0955--0674(99)80032-5
58. Stoian A, Rowland RRR, Petrovan V, Sheahan M, Samuel MS, Whitworth KM, Wells KD, Zhang J, Beaton B, Cigan M, Prather RS. 2020. The use of cells from ANPEP knockout pigs to evaluate the role of aminopeptidase N (APN) as a receptor for porcine deltacoronavirus (PDCoV). Virology 541:136–140. https://doi.org/10.1016/j.virol.2019.12.007
59. Wang B, Liu Y, Ji C-M, Yang Y-L, Liang Q-Z, Zhao P, Xu L-D, Lei X-M, Luo W-T, Qin P, Zhou J, Huang Y-W, Gallagher T. 2018. Porcine deltacoronavirus engages the transmissible gastroenteritis virus functional receptor porcine aminopeptidase N for infectious cellular entry. J Virol 92. https://doi.org/10.1128/JVI.00318-18
60. Yang Y-L, Liu J, Wang T-Y, Chen M, Wang G, Yang Y-B, Geng X, Sun M-X, Meng F, Tang Y-D, Feng L. 2021. Aminopeptidase N is an entry co-factor triggering porcine deltacoronavirus entry via an endocytotic pathway. J Virol 95:e0094421. https://doi.org/10.1128/JVI.00944-21
61. Zhu X, Liu S, Wang X, Luo Z, Shi Y, Wang D, Peng G, Chen H, Fang L, Xiao S. 2018. Contribution of porcine aminopeptidase N to porcine deltacoronavirus infection. Emerg Microbes Infect 7:65. https://doi.org/10.1038/s41426-018-0068-3
62. Kim DS, Son KY, Koo KM, Kim JY, Alfajaro MM, Park JG, Hosmillo M, Soliman M, Baek YB, Cho EH, Lee JH, Kang MI, Goodfellow I, Cho KO. 2016. Porcine sapelovirus uses α2,3-linked sialic acid on GD1A ganglioside as a receptor. J Virol 90:4067–4077. https://doi.org/10.1128/JVI.02449-15
63. Twu W-I, Lee J-Y, Kim H, Prasad V, Cerikan B, Haselmann U, Tabata K, Bartenschlager R. 2021. Contribution of autophagy machinery factors to HCV and SARS-CoV-2 replication organelle formation. Cell Rep 37:110049. https://doi.org/10.1016/j.celrep.2021.110049
64. Li S, Xu C, Fu Y, Lei PJ, Yao Y, Yang W, Zhang Y, Washburn MP, Florens L, Jaiswal M, Wu M, Mohan M. 2018. DYRK1A interacts with histone acetyl transferase p300 and CBP and localizes to enhancers. Nucleic Acids Res 46:11202–11213. https://doi.org/10.1093/nar/gky754
65. Sitz JH, Tigges M, Baumgärtel K, Khaspekov LG, Lutz B. 2004. DYRK1A potentiates steroid hormone-induced transcription via the chromatin remodeling factor Arip4. Mol Cell Biol 24:5821–5834. https://doi.org/10.1128/MCB.24.13.5821-5834.2004
66. Di Vona C, Bezdan D, Islam A, Salichs E, López-Bigas N, Ossowski S, de la Luna S. 2015. Chromatin-wide profiling of DYRK1A reveals a role as a gene-specific RNA polymerase II CTD kinase. Mol Cell 57:506–520. https://doi.org/10.1016/j.molcel.2014.12.026
67. Kelly PA, Rahmani Z. 2005. DYRK1A enhances the mitogen-activated protein kinase cascade in PC12 cells by forming a complex with Ras, B-Raf, and MEK1. Mol Biol Cell 16:3562–3573. https://doi.org/10.1091/mbc.e04-12-1085
68. Prentice E, Jerome WG, Yoshimori T, Mizushima N, Denison MR. 2004. Coronavirus replication complex formation utilizes components of cellular autophagy. J Biol Chem 279:10136–10141. https://doi.org/10.1074/jbc.M306124200
69. Miller K, McGrath ME, Hu Z, Ariannejad S, Weston S, Frieman M, Jackson WT. 2020. Coronavirus interactions with the cellular autophagy machinery. Autophagy 16:2131–2139. https://doi.org/10.1080/15548627.2020.1817280
70. Ou X, Qian Z. 2023. Characterization of SARS-Cov-2 glycoprotein using a quantitative cell–cell fusion system, p 179–186. In Aquino de Muro M (ed), Virus-host interactions: methods and protocols. Springer US, New York, NY.